Structural Engineering and Mechanics, *Vol. 68*, *No. 2 (2018) 183-191*
DOI: https://doi.org/10.12989/sem.2018.68.2.183

Dynamic stiffness formulations for harmonic response of infilled frames

Baran Bozyigit* and Yusuf Yesilce[a]

Department of Civil Engineering, Dokuz Eylul University, 35160, Buca, Izmir, Turkey

(Received May 1, 2018, Revised August 10, 2018, Accepted August 17, 2018)

Abstract. In this paper, harmonic responses of infilled multi-storey frames are obtained by using a single variable shear deformation theory (SVSDT) and dynamic stiffness formulations. Two different planar frame models are used which are fully infilled and soft storey. The infill walls are modeled by using equivalent diagonal strut approach. Firstly, free vibration analyses of bare frame and infilled frames are performed. The calculated natural frequencies are tabulated with finite element solution results. Then, harmonic response curves (HRCs) of frame models are plotted for different infill wall thickness values. All of the results are presented comparatively with Timoshenko beam theory results to reveal the effectiveness of SVSDT which considers the parabolic shear stress distribution along the frame member cross-sections.

Keywords: dynamic stiffness; harmonic response; infilled frame; natural frequency; single variable shear deformation theory

1. Introduction

Dynamic response analysis and resonance phenomenon have been an interesting research area for civil engineering applications. The analysis of exact dynamic behaviour of frame structures is a challenging task for safe design especially against earthquakes. The exact vibration analyses of frames are performed via distributed parameter model approach. Due to complicated and time consuming analysis procedure, limited studies about exact free vibrations of frames can be found in open literatures. Mei (2012) performed free vibration analysis of one storey frames by using wave vibration approach according to Euler-Bernoulli beam theory (EBT). Grossi and Albarracin (2013) obtained natural frequencies of inclined frames by variational approach. Labib *et al*. (2014) applied dynamic stiffness formulation for free vibrations of cracked frames using EBT. Mei and Sha (2015) presented an application of wave propagation for vibrations of a spatial frame using EBT. Mei (2018) calculated modes and frequency response of frames using EBT and Timoshenko beam theory (TBT) via wave vibration approach. Banerjee and Ananthapuvirajah (2018) obtained natural frequencies of single-bay single-story portal frames via the dynamic stiffness method (DSM). Bozyigit and Yesilce (2018) performed free vibration analysis of planar frames using DSM according to SVSDT.

Dynamic response of structures such as beams, beam assembly structures and shells are investigated using distributed parameter model in several studies. Li *et al.* (2016) derived dynamic stiffness formulations for in-plane, bending vibrations and harmonic response of plates. Free vibrations and dynamic response of cross-ply laminated shells are investigated via DSM by Thinh and Nguyen (2016). Han *et al.* (2017) investigated forced vibrations of bending-torsion coupled Timoshenko beams using Green’s function. Attar *et al*. (2017) obtained dynamic response of cracked Timoshenko beams on elastic foundations under moving harmonic loads. Tan *et al*. (2018) investigated dynamic response of non-uniform Timoshenko beams with elastic supports under a moving spring-mass system. Ai and Ren (2017) obtained dynamic response analysis of an infinite Euler-Bernoulli beam supported by a transversely isotropic multilayered half-space under moving loads. Miao *et al.* (2018) obtained closed-form solution of dynamic response of an infinite Euler-Bernoulli beam on elastic foundation under harmonic line load.

The infill walls have been extensively used in the building type frame structures as separators or architectural reasons. However, the effects of infill walls on behavior of frame structures are neglected in general as analyses of bare frames are significantly practical when compared to analyses of infilled frames. Thus, the mathematical modeling of infill walls has been an attractive research field. Polyakov (1950) presented the first study about effects of infill walls for analysis of structures. The infill is modeled using an equivalent pin-jointed diagonal strut by Holmes (1961). In this study, the material properties of strut are same as infill’s. In literature, the variations of equaivalent strut approach can be found (Holmes 1963, Mainstone 1974, El-Dakhakhni *et al.* 2003). The equivalent diagonal strut model which is also called as macro-model, is added to several codes such as Eurocode-6 (1996) and FEMA-356 (2000). Dynamic analysis of infilled frames are performed in limited studies. Chaker and Cherifati (1999) measured frequencies of an infilled frame building and bare frame building. In this study, it is concluded that

*Corresponding author, Ph.D. Candidate
E-mail: baran.bozyigit@deu.edu.tr
[a]Associate Professor
E-mail: yusuf.yesilce@deu.edu.tr

http://www.techno-press.com/journals/sem&subpage=7
ISSN: 1225-4568 (Print), 1598-6217 (Online)

fundamental frequency of infilled frame building is much higher than bare frame building. Thambiratnam (2009) obtained fundamental period of a simple frame structure using finite element method (FEM). Tamboli and Karadi (2012) applied equivalent diagonal strut method to seismic analysis of 3D frames via ETABS. Salama (2015) investigated calculation of period of concrete moment resisting frame buildings. Beiraghi (2016) calculated fundamental period of steel frame buildings via equivalent diagonal strut approach and ETABS. Al-Balhawi and Zhang (2017) obtained elastic vibration periods of reinforced concrete frames with various infill walls by using SAP2000. Ozturkoglu e*t al.* (2017) performed nonlinear response analysis of RC frames considering masonary infill walls with openings.

The cross-sections of Euler-Bernoulli beams behave rigid and remain perpendicular to the neutral axis under bending. Thus, natural frequencies of beams are overestimated according to EBT. More realistic results of dynamic analyses can be obtained by using TBT which takes shear deformation and rotational inertia into account. However, formulations of TBT are strictly related to a parameter called shear coefficient or area reduction factor which is used for decreasing the error arised from assumption of constant shear stress distribution on the cross section (Han *et al.* 1999). This situation canalized researchers to develop high-order beam theories that consider a realistic shear stress distribution with the assumption of cross section does not remain plane after bending (Levinson 1981, Bickford 1982, Reddy 1984, Heyliger and Reddy 1988). Ghugal and Shimpi (2001) compared EBT, TBT and high-order beam theories for isotropic and anisotropic beams. Shimpi (2002) studied on a refined plate theory that based on shear and bending components of lateral and axial displacements. Shimpi *et al.* (2007) introduced two displacement based shear deformation theories involving only two unknown functions for plate bending. Even high-order theories provide more accurate results when compared to EBT and TBT, the formulations of high-order beam theories are significantly complicated and time-consuming. Shimpi *et al.* (2017) presented a new SVSDT that considers the parabolic shear stress distribution along the cross-section. The governing equation of motion of SVSDT is a fourth order partial differential equation. Moreover, the shear correction factor is not needed according to SVSDT. Klouche *et al.* (2017) applied an original SVSDT to buckling analysis of thick isotropic plates. Abdelbari *et al*. (2018) studied on a single variable shear deformation model for bending analysis of thick isotropic beams.

An effective method is necessary for exact vibration problems of beam assembly structures like frames because of numerous complicated formulations. The DSM is a suitable method as analysis procedure can be extended by a standard coding technique for structures that have multiple members such as frames. The DSM provides exact results as uses the exact mode shapes (Banerjee 1997). There are many studies in literature about application of DSM for various types of structures under different boundary conditions (Damanpack and Khalili 2012, Ghandi *et al.* 2012, Banerjee and Jackson 2013, Tounsi *et al*. 2014, Su and Banerjee 2015, Bozyigit and Yesilce 2016, Naprstek and Fischer 2017, Ghandi and Shiri 2017, Howson and Watson 2017, Banerjee and Ananthapuvirajah 2018, Zhang *et al.* 2018).

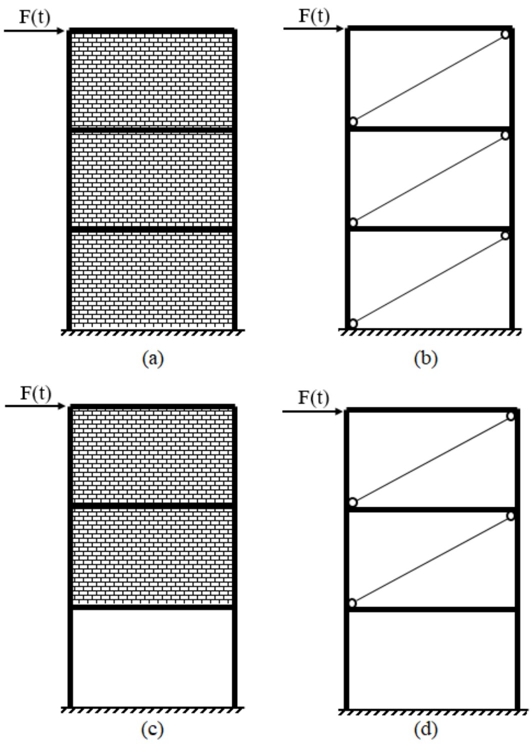

Fig. 1 Infilled planar frames and mathematical models

The novelty of this study is based on calculating exact dynamic response of frames considering infill walls for the first time. The natural frequencies and HRCs of fully infilled and soft storey frame models are obtained using DSM for different infill thickness values. The HRCs reveal the natural frequencies of infilled frames directly. The effects of using SVSDT instead of TBT on dynamic response analysis of infilled are observed. The results are obtained from algorithms that prepared in Matlab.

2. Model and theory

In this study, a single-bay three-storey fixed supported planar frame is considered. The schematic view of fully infilled model and soft storey model are presented in Figs. 1(a) and (c), respectively. The infill walls are modeled by means of equivalent pin-jointed diagonal strut method (Figs. 1(b)-(d)). In Fig. 1, F(t) represents a sinusoidal dynamic point load.

The Young's modulus and thickness values of diagonal struts are taken same as infill's. The width of the strut is defined as (FEMA-356 2000)

$$\lambda = \sqrt[4]{\frac{E_{in} t_{in} \sin(2\varphi)}{4EI_c h_{in}}} \tag{1}$$

where λ is a coefficient for calculation of equivalent width of infill strut, E_{in} is Young's modulus of infill, E is Young's modulus of beams and columns, t_{in} and h_{in} are the thickness

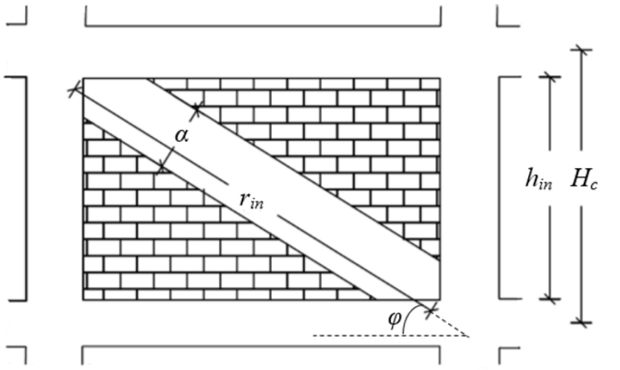

Fig. 2 Parameters of formulations of equivalent diagonal strut approach

and height of infill wall, respectively, φ is the angle between diagonal strut and horizontal plane, I_c is moment of inertia of columns. The equivalent width of the strut is written as Eq. (2) by using λ

$$\alpha = 0.175(\lambda H_c)^{-0.4} r_{in} \tag{2}$$

where α is width of the strut and r_{in} is length of the strut.

Eqs. (1) and (2) present widely used macro-modeling parameters of infills. The equivalent width of the strut α is obtained after calculating λ which is a function of infill-to-frame stiffness parameter.

The parameters of infill wall are presented in Fig. 2.

The following assumptions are considered in this study:

1) The material of frame members and equivalent struts are isotropic.

2) The frame members and struts behave linear and elastic.

3) The effect of damping is ignored.

The transverse deflection function of a beam according to SVSDT is defined in Eq. (3) (Shimpi *et al.* 2017)

$$y^S = y_b + y_s \tag{3}$$

where y^S is total transverse displacement, y_b is displacement component of bending and y_s is displacement component of shearing. The governing equation of motion of a beam in free vibration according to SVSDT is given as follows (Shimpi *et al.* 2017)

$$\begin{aligned} &EI\frac{\partial^4 y_b}{\partial x^4} - \frac{\bar{m}I}{A}\left(1+\frac{12(1+\mu)}{5}\right)\frac{\partial^4 y_b}{\partial x^2 \partial t^2} \\ &+\bar{m}\frac{\partial^2 y_b}{\partial t^2} + \frac{\bar{m}^2 I}{A^2 E}\frac{12(1+\mu)}{5}\frac{\partial^4 y_b}{\partial t^4} = 0 \end{aligned} \tag{4}$$

where A is cross-sectional area, μ is Poisson's ratio, $\bar{m}$ is mass per unit length, I is area moment of inertia, t is time. y_b is obtained from the solution of Eq. (4). Eq. (5) is written using separation of variables method with the assumption of $y_b(x,t) = y_b(x)e^{i\omega t}$ where ω is angular frequency.

$$A_0 \frac{d^4 y_b}{dz^4} + B_0 w^2 \frac{d^2 y_b}{dz^2} - C_0 w^2 y_b(z) + D_0 w^4 y_b(z) = 0$$

where

$$\begin{aligned} &A_0 = \frac{EI}{L^4}; B_0 = -\frac{\bar{m}I}{AL^2}\left(1+\frac{12(1+\mu)}{5}\right); C_0 = \bar{m}; z = x/L \\ &D_0 = \frac{\bar{m}^2 I}{A^2 E}\frac{12(1+\mu)}{5} \end{aligned} \tag{5}$$

The solution of $y_b(z)$ can be written as

$$y_b(z) = \{D\}e^{ikz} \tag{6}$$

The bending component of transverse displacement function is achieved by substituting Eq. (6) into Eq. (5)

$$y_b(z) = (D_1 e^{ik_1 z} + D_2 e^{ik_2 z} + D_3 e^{ik_3 z} + D_4 e^{ik_4 z}) \tag{7}$$

where k_n (n:1,2,3,4) are characteristic roots of the equation that obtained by substituting Eq. (6) into Eq. (5).

The bending component of slope function can be written as follows

$$\frac{dy_b}{dz} = (ik_1 D_1 e^{ik_1 z} + ik_2 D_2 e^{ik_2 z} + ik_3 D_3 e^{ik_3 z} + ik_4 D_4 e^{ik_4 z}) \tag{8}$$

The bending moment function and shear force function according to SVSDT are defined in Eqs. (9) and (10), respectively (Shimpi *et al.* 2017).

$$M^S(z) = -\frac{EI}{L^2}\frac{d^2 y_b}{dz^2} \tag{9}$$

$$Q^S(z) = -\frac{EI}{L^3}\frac{d^3 y_b}{dz^3} - \frac{\bar{m}I\omega^2}{AL}\frac{dy_b}{dz} \tag{10}$$

Eqs. (9)-(10) can be rewritten as Eqs. (11)-(12) using Eq. (7)

$$M^S(z) = (Hk_1^2 D_1 e^{ik_1 z} + Hk_2^2 D_2 e^{ik_2 z} + Hk_3^2 D_3 e^{ik_3 z} + Hk_4^2 D_4 e^{ik_4 z}) \tag{11}$$

$$\begin{aligned} Q^S(z) = &(Jik_1^3 - Kik_1)D_1 e^{ik_1 z} + (Jik_2^3 - Kik_2)D_2 e^{ik_2 z} \\ &+(Jik_3^3 - Kik_3)D_3 e^{ik_3 z} + (Jik_4^3 - Kik_4)D_4 e^{ik_4 z} \end{aligned} \tag{12}$$

where $H = EI/L^2, J = EI/L^3, K = (\bar{m}I\omega^2)/(AL)$

The shearing component of displacement and total displacement functions are written in Eqs. (13) and (14), respectively.

$$y_s = T\left(-H\frac{d^2 y_b}{dz^2} - Py_b(z)\right) \tag{13}$$

$$\begin{aligned} y^S = &(THk_1^2 - TP + 1)D_1 e^{ik_1 z} + (THk_2^2 - TP + 1)D_2 e^{ik_2 z} \\ &+ (THk_3^2 - TP + 1)D_3 e^{ik_3 z} + (NHk_4^2 - TP + 1)D_4 e^{ik_4 z} \end{aligned} \tag{14}$$

where $T = \dfrac{12(1+\mu)}{5AE}; P = (\bar{m}I\omega^2/A)$

The total slope function is obtained as assembly of $\dfrac{dy_b}{dz}$ and $\dfrac{dy_s}{dz}$

$$\frac{dy^S}{dz} = \left(ik_1 + TJik_1^3 - TRik_1\right)D_1e^{ik_1z} + \left(ik_2 + TJik_2^3 - TRik_2\right)D_2e^{ik_2z} + \left(ik_3 + TJik_3^3 - TRik_3\right)D_3e^{ik_3z} + \left(ik_4 + TJik_4^3 - TRik_4\right)D_4e^{ik_4z} \tag{15}$$

where $R=P/L$

The axial vibrations are not neglected in this study. The governing equation of motion of a beam in free axial vibration is given in Eq. (16) (Rao 1995)

$$AE\frac{\partial^2 u(x,t)}{\partial x^2} - \bar{m}\frac{\partial^2 u(x,t)}{\partial t^2} = 0 \tag{16}$$

where $u(x,t)$ is axial displacement function. By applying separation of variables method to Eq. (16) using $u(x,t)=u(x)e^{i\omega t}$ with the assumption of harmonic motion, Eq.(17) is obtained.

$$\frac{d^2u(z)}{dz^2} + \frac{\bar{m}\omega^2L^2}{AE}u(z) = 0 \tag{17}$$

Substituting Eq. (18) into Eq. (17), the axial displacement function $u(z)$ and axial force function $N(z)$ are achieved as Eqs. (19)-(20), respectively.

$$u(z) = \{D\}e^{ikz} \tag{18}$$

$$u(z) = (D_5e^{ik_5z} + D_6e^{ik_6z}) \tag{19}$$

$$N(z) = V(ik_5D_5e^{ik_5z} + ik_6D_6e^{ik_6z}) \tag{20}$$

where $V = AE/L$ and k_n (n:5, 6) are characteristic roots of the equation that obtained by substituting Eq. (18) into (Eq. (17)).

3. Dynamic stiffness formulations

The dynamic stiffness formulations of frames are derived by using end forces and end displacements of frame members. The global dynamic stiffness matrix a frame can be constructed when all of the global member dynamic stiffness matrices are achieved. The vector of end displacements of a frame member and the vector of coefficients for SVSDT are presented in Eqs. (21)-(22), respectively.

$$\delta^S = [u_0 \quad y_0^S \quad \theta_0^S \quad u_1 \quad y_1^S \quad \theta_1^S]^T \tag{21}$$

$$D = [D_1 \quad D_2 \quad D_3 \quad D_4 \quad D_5 \quad D_6]^T \tag{22}$$

where

$$u_0 = u(z=0), y_0^S = y^S(z=0), \theta_0^S = \theta^S(z=0),$$
$$u_1 = u(z=1), y_1^S = y_1(z=1), \theta_1^S = \theta^S(z=1)$$

Eq. (23) can be written by using Eqs. (14)-(15) and (19) as

$$\delta^S = \Delta^S D \tag{23}$$

where

$$\Delta^S = \begin{bmatrix} 0 & 0 & 0 & 0 & 1 & 1 \\ \lambda_1^S & \lambda_2^S & \lambda_3^S & \lambda_4^S & 0 & 0 \\ \eta_1^S & \eta_2^S & \eta_3^S & \eta_4^S & 0 & 0 \\ 0 & 0 & 0 & 0 & e^{ik_5} & e^{ik_6} \\ \lambda_1^S e^{ik_1} & \lambda_2^S e^{ik_2} & \lambda_3^S e^{ik_3} & \lambda_4^S e^{ik_4} & 0 & 0 \\ \eta_1^S e^{ik_1} & \eta_2^S e^{ik_2} & \eta_3^S e^{ik_3} & \eta_4^S e^{ik_4} & 0 & 0 \end{bmatrix}$$

$$\lambda_n^S = \left(THk_n^2 - TP + 1\right), \eta_n^S = \left(ik_n + TJik_n^3 - TRik_n\right), (n = 1,2,3,4)$$

The vector of end forces F^S of the frame members is written as follows

$$F^S = [N_0 \quad Q_0^S \quad M_0^S \quad N_1 \quad Q_1^S \quad M_1^S]^T \tag{24}$$

where

$$N_0 = N(z=0), Q_0^S = Q^S(z=0), M_0^S = M^S(z=0),$$
$$N_1 = N(z=1), Q_1^S = Q^S(z=1), M_1^S = M^S(z=1)$$

The following sign convention is considered

$$N_0 = -N_1, \quad Q_0^S = -Q_1^S, \quad M_0^S = -M_1^S \tag{25}$$

Eq. (26) can be written by using Eqs. (11)-(12) and (20) as

$$F^S = \kappa^S D \tag{26}$$

where

$$\kappa^S = \begin{bmatrix} 0 & 0 & 0 & 0 & Vik_5 & Vik_6 \\ \Lambda_1^S & \Lambda_2^S & \Lambda_3^S & \Lambda_4^S & 0 & 0 \\ \Psi_1^S & \Psi_2^S & \Psi_3^S & \Psi_4^S & 0 & 0 \\ 0 & 0 & 0 & 0 & -Vik_5e^{ik_5} & -Vik_6e^{ik_6} \\ -\Lambda_1^S e^{ik_1} & -\Lambda_2^S e^{ik_2} & -\Lambda_3^S e^{ik_3} & -\Lambda_4^S e^{ik_4} & 0 & 0 \\ -\Psi_1^S e^{ik_1} & -\Psi_2^S e^{ik_2} & -\Psi_3^S e^{ik_3} & -\Psi_4^S e^{ik_4} & 0 & 0 \end{bmatrix}$$

$$\Lambda_n^S = (Jik_n^3 - Kik_n), \Psi_n^S = Hk_n^2, (n = 1,2,3,4)$$

Eq. (27) is obtained by using relation between Eqs. (23) and (26).

$$F^S = \kappa^S (\Delta^S)^{-1} \delta^S \tag{27}$$

$$K^{*S} = \kappa^S (\Delta^S)^{-1} \tag{28}$$

In Eq. (28), K^{*S} represents the local dynamic stiffness matrix of a frame member according to SVSDT. The global dynamic stiffness matrix of a frame member is obtained by transforming the local member dynamic stiffness matrix to global member dynamic stiffness matrix. The transformation matrix and global dynamic stiffness matrix of a frame member are presented in Eqs. (29)-(30), respectively (Paz and Leigh 2004).

$$TM = \begin{bmatrix} cos(\Omega) & sin(\Omega) & 0 & 0 & 0 & 0 \\ -sin(\Omega) & cos(\Omega) & 0 & 0 & 0 & 0 \\ 0 & 0 & 1 & 0 & 0 & 0 \\ 0 & 0 & 0 & cos(\Omega) & sin(\Omega) & 0 \\ 0 & 0 & 0 & -sin(\Omega) & cos(\Omega) & 0 \\ 0 & 0 & 0 & 0 & 0 & 1 \end{bmatrix} \tag{29}$$

$$\bar{K}^{*S} = (TM)^{-1}(K^{*S})(TM) \tag{30}$$

In Eq. (29), Ω represents the angle between local axes of the frame member and global axes of the frame.

The equivalent pin-jointed diagonal struts vibrate only in axial direction. Therefore, the local dynamic stiffness matrix of diagonal struts K_{in} can be given as (Paz and Leigh 2004)

$$K_{in} = E_{in}A_{in}\beta\begin{bmatrix} \cot\beta r_{in} & -\operatorname{cosec}\beta r_{in} \\ -\operatorname{cosec}\beta r_{in} & \cot\beta r_{in} \end{bmatrix} \tag{31}$$

where A_{in} is cross-sectional area of equivalent diagonal strut, β equals to $\sqrt{m_{in}\omega^2 / E_{in}A_{in}}$ considering m_{in} as mass per unit length of diagonal strut.

The diagonal struts are pin-jointed at nodes that have 2 degrees of freedom in vertical and horizontal directions. Eq. (31) is used to obtain global dynamic stiffness matrix of diagonal strut K^{*}_{in} as

$$K^{*}_{in} = \begin{bmatrix} \cot\beta r_{in}\cos\varphi & 0 & -\operatorname{csc}\beta r_{in}\cos\varphi & 0 \\ 0 & \cot\beta r_{in}\sin\varphi & 0 & -\operatorname{csc}\beta r_{in}\sin\varphi \\ -\operatorname{csc}\beta r_{in}\cos\varphi & 0 & \cot\beta r_{in}\cos\varphi & 0 \\ 0 & -\operatorname{csc}\beta r_{in}\sin\varphi & 0 & \cot\beta r_{in}\sin\varphi \end{bmatrix} \tag{32}$$

The global dynamic stiffness matrices of frames can be obtained by a standard coding technique via Eqs. (30) and (32) for SVSDT. The global dynamic stiffness matrix of frames are reduced due to zero displacements at fixed support joints. Thus, the ω values that equate the reduced global dynamic stiffness matrices of the frames are obtained as natural frequencies using Wittrick-Williams algorithm. Furthermore, a method that based on a trial and error on interpolation can be used for calculating roots. When there is a sign change between trial values, there must be a root lying in this interval. (Bozyigit and Yesilce 2018).

It should be noted that formulations of well known Timoshenko beams are not presented to simplify the paper. The DSM applications of different types of Timoshenko beams under various boundary conditions can be investigated for further information (Su and Banerjee 2015, Deng *et al*. 2017, Han *et al*. 2018).

The HRCs that represent the relationship between logarithmic scaled displacement and forcing frequency can be obtained by using Eq. (27). Besides observation of dynamic response due to a harmonic loading, the HRCs are efficient tools for free vibrations as peaks of curves represent natural frequencies directly. Thus, HRCs remove the necessity of root finding methods such as Wittrick-Williams algorithms when natural frequencies are searched (Thinh and Nguyen 2016). A schematic view of a harmonic response curve is presented in Fig. 3 where δ is displacement value, $\bar{\omega}$ is forcing frequency, ω_1 and ω_2 are first two natural frequencies, ω_{ARF1} and ω_{ARF2} are first two anti-resonant frequencies (ARFs).

The ARFs are useful dynamic parameters that become important on behaviour of nonstructural elements under excitation. The response of elements diminishes to zero when the forcing frequency is near an ARF. The peaks and valleys of a logarithmic scaled harmonic response curve shows natural frequencies and ARFs, respectively (Lien and Yao 2000). The ARFs are also used by researchers on crack detection and finite element model updating (Jones and Turcotte 2002, Dilena and Morassi 2004, Hanson *et al.* 2007, Rubio *et al.* 2015).

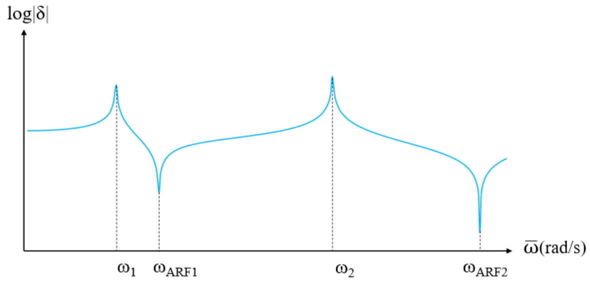

Fig. 3 Shematic view of logarithmic scaled harmonic response curve

Table 1 First three natural frequencies of bare frame model

ω(rad/s)	TBT	SVSDT	ANSYS
1st	31.2758	28.39940	31.6120
2nd	107.7087	101.3153	108.3598
3rd	205.2537	201.8114	205.4225

Table 2 First three natural frequencies of infilled frames for different wall thickness values

	t_{in} (cm)	ω (rad/s)	TBT	SVSDT	ANSYS
Soft		1st	37.3879	34.8892	35.7526
Story		2nd	127.9294	120.1342	121.6110
Frame		3rd	234.7838	226.4529	224.7056
Fully	10	1st	42.1982	38.8298	38.9199
Infilled		2nd	134.1800	125.5259	125.6637
Frame		3rd	236.1210	227.8360	224.7056
Soft		1st	38.6015	36.3298	36.7208
Story		2nd	134.7135	126.5661	126.2920
Frame		3rd	246.0921	236.1763	231.9124
Fully	15	1st	45.4947	42.0196	41.2711
Infilled		2nd	142.9009	133.7190	131.6641
Frame		3rd	247.4648	237.7093	232.0380
Soft		1st	39.3598	37.3092	37.3724
Story		2nd	140.4562	132.0544	130.3321
Frame		3rd	256.1729	244.9792	238.7045
Fully	20	1st	48.1794	44.6425	43.2214
Infilled		2nd	150.1953	140.6618	136.7787
Frame		3rd	257.4055	246.5022	238.5663

4. Numerical examples and discussions

The numerical examples of the study include free and forced vibration analyses of bare frame and infilled single-bay three-storey frames. The numerical analyses of the study are performed based on the following data:

• Unit weight of frame members = 24.525 kN/m^3

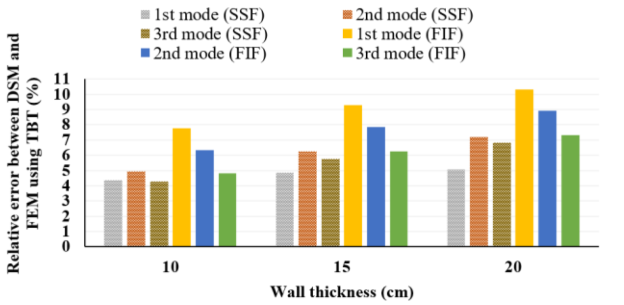

Fig. 4 Relative error between DSM and FEM results for TBT

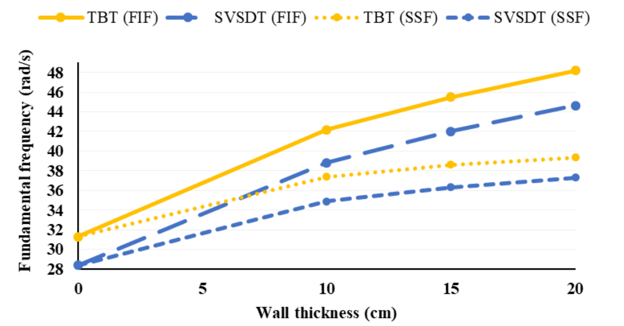

Fig. 5 Increment of fundamental frequencies of infilled frames by means of DSM

- Unit weight of infill walls = 7.85 kN/m^3
- Young's modulus of frame members = 2.94x10^7 kN/m^2
- Young's modulus of infill walls = 9.81x10^5 kN/m^2
- Poisson's ratio of frame members = 0.2
- Height of the columns = 3.5 m
- Length of the beams = 5 m
- Cross-sectional area of the columns = 0.15 m^2
- Cross-sectional area of the beams = 0.125 m^2
- Moment of inertia of the columns = 3.125x10^{-3} m^4
- Moment of inertia of the beams = 2.604x10^{-3} m^4
- Shear correction for TBT, $\bar{k}$ = 1.2
- F(t) = 20sin($\overline{\omega}$t)

Using DSM and FEM (ANSYS), the first three natural frequencies of bare frame and infilled frame models are presented in Tables 1-2, respectively.

It is seen from Table 1 that SVSDT provides slightly lower natural frequencies in comparison with TBT for bare frame model. The DSM and FEM solutions are in very well agreement for bare frame. It should be noted that ANSYS performs finite element analysis according to TBT and frame elements are divided into 50 elements in this study. Table 2 shows that natural frequencies of infilled frame models using TBT are overestimated according to SVSDT results. Moreover, the agreement of ANSYS and DSM solutions is decreased when infill walls are taken into account. The relative error between DSM and ANSYS results can be observed from Fig. 4 where SSF and FIF denote soft storey frame and fully infilled frame, respectively. For infilled frame models, an augmentation of natural frequencies is arised with increasing wall thickness value for all modes. The increment of fundamental frequencies by considering infills is plotted in Fig. 5.

In the forced vibration analyses part of numerical

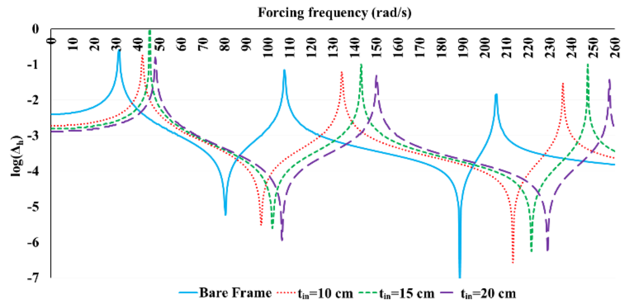

Fig. 6 HRCs of Δ_h for fully infilled frame model according to TBT

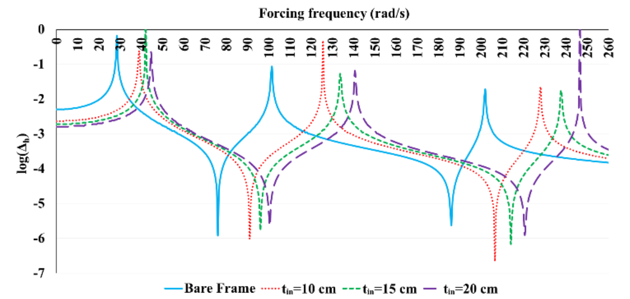

Fig. 7 HRCs of Δ_h for fully infilled frame model according to SVSDT

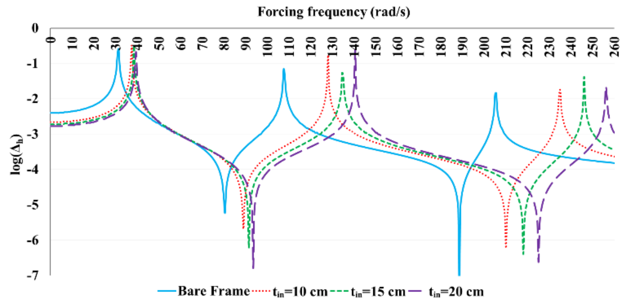

Fig. 8 HRCs of Δ_h for soft storey frame model according to TBT

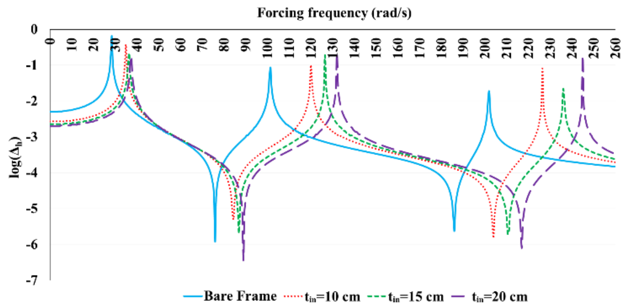

Fig. 9 HRCs of Δ_h for soft storey frame model according to SVSDT

examples, the HRCs of frame models are plotted for horizontal displacement of node under dynamic load (Δ_h). For different wall thickness values, the harmonic responses of fully infilled frame model using TBT and SVSDT are presented in Figs. 6 and 7, respectively. Similarly, the HRCs of soft storey frame are obtained for different wall thickness values according to TBT and SVSDT (Figs. 8 and 9).

Figs. 6-9 show that peak and valley locations of

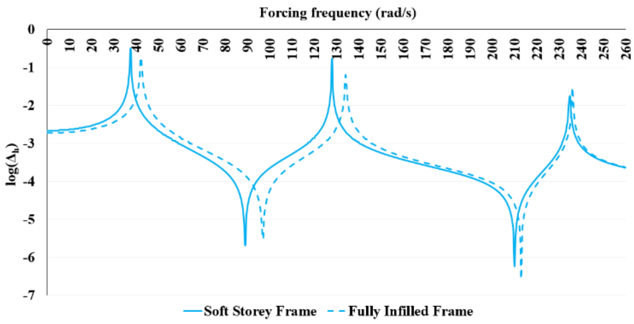

Fig. 10 HRCs of Δ_h for frame models using TBT (t_{in} = 10 cm)

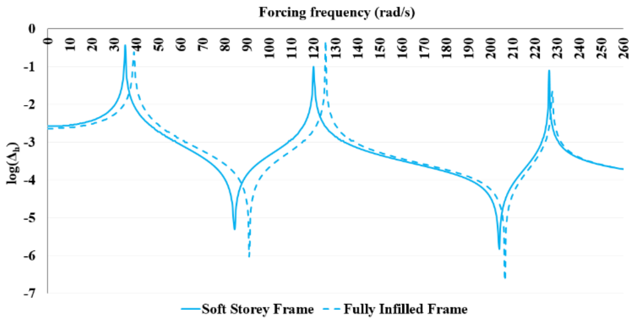

Fig. 11 HRCs of Δ_h for frame models using SVSDT (t_{in} = 10 cm)

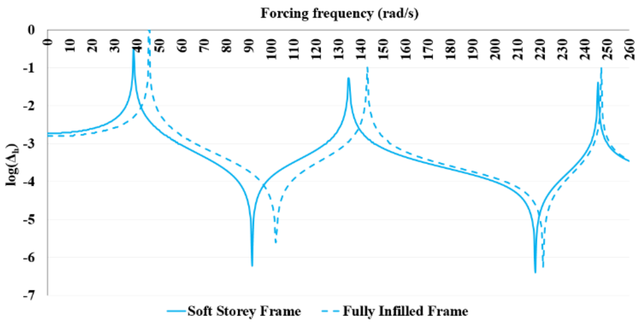

Fig. 12 HRCs of Δ_h for frame models using TBT (t_{in} = 15 cm)

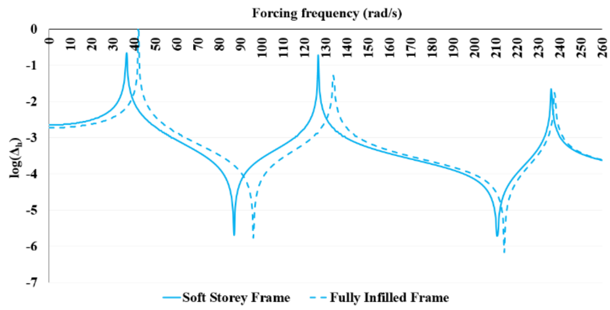

Fig. 13 HRCs of Δ_h for frame models using SVDST (t_{in} = 15 cm)

harmonic response curves are shifted positively with increasing lateral stiffness of frame as a result of augmentation of infill wall thickness.

By taking t_{in} as 10 cm, the harmonic responses of soft storey and infilled frames are presented comparatively for TBT and SVSDT in Figs. 10 and 11, respectively. The

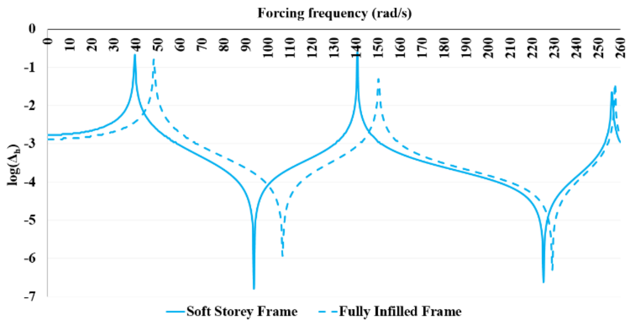

Fig. 14 HRCs of Δ_h for frame models using TBT (t_{in} = 20 cm)

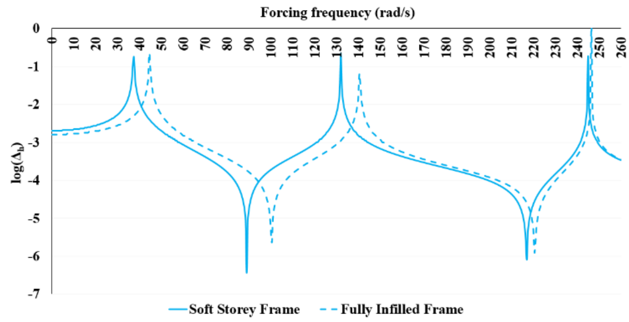

Fig. 15 HRCs of Δ_h for infilled frame models using SVSDT (t_{in} = 20 cm)

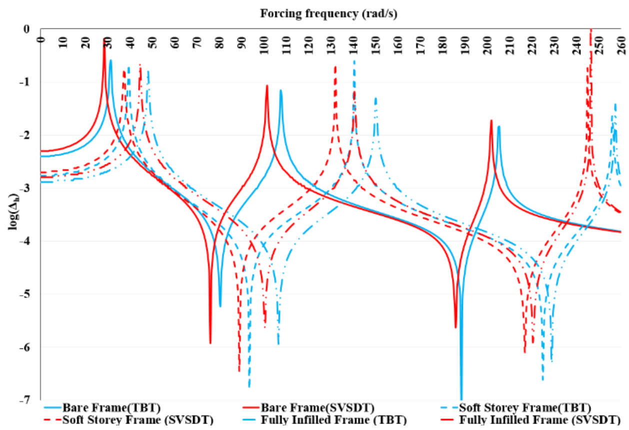

Fig. 16 HRCs of Δ_h for all frame models using TBT and SVSDT (t_{in} = 20 cm)

HRCs of infilled frame models for t_{in} = 15 cm and t_{in} = 20 cm are presented in Figs. 12-13 and Figs. 14-15, respectively. Fig.16 represents HRCs of all frame models comparatively using TBT and SVSDT for t_{in} = 20 cm.

According to Figs. 10-15, resonant and anti-resonant frequency values of fully infilled frame model are higher in comparison with soft story frame model. Fig. 16 reveals that SVSDT provides lower resonant frequencies and ARFs when compared to TBT for infilled frames.

5. Conclusions

In this study, the effects of infill walls on dynamic behaviour of frames are revealed by means of dynamic stiffness formulations. A realistic beam theory called

SVSDT which considers parabolic shear stress distribution along the cross-section is used with well known TBT. The numerical analyses are performed for different wall thickness values and two types of planar frames which are soft storey and fully infilled models. The natural frequencies are detected as resonant frequencies from HRCs without using any root finding algorithm of DSM procedures. The results of SVSDT are tabulated with TBT results. The importance of considering infill walls on dynamic analysis of frame structures is highlighted by results of several numerical examples.

References

Abdelbari, S., Amar, L.H.H., Kaci, A. and Tounsi, A. (2018), "Single variable shear deformation model for bending analysis of thick beams", *Struct. Eng. Mech.*, **67**(3), 291-300.

Ai, Z.H. and Ren, G.P. (2017), "Dynamic response of an infinite beam on a transversely isotropic multilayered half-space due to a moving load", *Int. J. Mech. Sci.*, **133**, 817-828.

Al-Balhawi, A. and Zhang, B. (2017), "Investigations of elastic vibration periods of reinforced concrete moment-resisting frame systems with various infill walls", *Eng. Struct.*, **151**, 173-187.

Attar, M., Karrech, A. and Regenauer-Lieb, K. (2017), "Dynamic response of cracked Timoshenko beams on elastic foundations under moving harmonic loads", *J. Vibr. Contr.*, **23**(3), 432-457.

Banerjee, J.R. (1997), "Dynamic stiffness for structural elements: A general approach", *Comput. Struct.*, **63**(1), 101-103.

Banerjee, J.R. and Ananthapuvirajah, A. (2018), "Free vibration of functionally graded beams and frameworks using the dynamic stiffness method", *J. Sound Vibr.*, **422**, 34-47.

Banerjee, J.R. and Jackson, D.R. (2013), "Free vibration of a rotating tapered Rayleigh beam: A dynamic stiffness method of solution", *Comput. Struct.*, **124**, 11-20.

Beiraghi, H. (2016), "Fundamental period of masonry infilled moment-resisting frame buildings", *Struct. Des. Tall Spec.*, **26**(5), 1-10.

Bickford, W.B. (1982), "A consistent higher order beam theory", *Develop. Theoret. Appl. Mech.*, **11**, 137-150.

Bozyigit, B. and Yesilce, Y. (2016), "Dynamic stiffness approach and differential transformation for free vibration analysis of a moving Reddy-Bickford beam", *Struct. Eng. Mech.*, **58**(5), 847-868.

Bozyigit, B. and Yesilce, Y. (2018) "Investigation of natural frequencies of multi-bay and multi-storey frames using single a variable shear deformation theory", *Struct. Eng. Mech.*, **65**(1), 9-17.

Chaker, A.A. and Cherifati, A. (1999), "Influence of masonary infill panels on the vibration and stiffness characteristics of R/C frame building", *Earthq. Eng. Struct. Dyn.*, **28**, 1061-1065.

Damanpack, A.R. and Khalili, S.M.R. (2012), "High-order free vibration analysis of sandwich beams with a flexible core using dynamic stiffness method", *Compos. Struct.*, **94**(5), 1503-1514.

Deng, H., Chen, K., Cheng, W. and Zhao, S. (2017), "Vibration and buckling analysis of double-functionally graded Timoshenko beam system on Winkler-Pasternac elastic foundation", *Compos. Struct.*, **160**, 152-168.

Dilena, M. and Morassi, A. (2004), "The use of antiresonances for crack detection in beams", *J. Sound Vibr.*, **276**, 195-214.

El-Dakhakhni W.W., Elgaaly, M. and Hamid, A.A. (2003), "Three-strut model for concrete masonary-infilled steel frames", *J. Struct. Eng.*, **129**(2), 177-185.

Eurocode 6 (1996), *Design of Masonry Structures-Part 1-1: General Rules for Reinforced and Unreinforced Masonry Structures*, European Committee for Standardization, Brussels, Belgium.

FEMA-356 (2000), *Prestandard and Commentary for the Seismic Rehabilitation of Buildings*, Federal Emergency Management Agency, Washington, U.S.A.

Ghandi, E. and Shiri, B. (2017), "On triply coupled vibration of eccentrically loaded thin-walled beam using dynamic stiffness matrix method", *Struct. Eng. Mech.*, **62**(6), 759-769.

Ghandi, E., Rafezy, B. and Howson, W.P. (2012), "On the bi-planar motion of a Timoshenko beam with shear resistant in-fill", *Int. J. Mech. Sci.*, **57**(1), 1-8.

Ghugal, Y.M. and Shimpi, R.P. (2001), "A review of refined shear deformation theories for isotropic laminated beams", *J. Reinf. Plast. Comp.*, **20**(3), 255-272.

Grossi, R.O. and Albarracin, C.M. (2013), "Variational approach to vibrations of frames with inclined members", *Appl. Acoust.*, **74**(3), 325-334.

Han, F., Dan, D. and Cheng, W. (2018), "An exact solution for dynamic analysis of a complex double-beam system", *Compos. Struct.*, **193**, 295-305.

Han, H., Cao, D. and Liu, L. (2017), "Green's functions for forced vibration analysis of bending-torsion coupled Timoshenko beam", *Appl. Math. Model.*, **45**, 621-635.

Han, S.M., Benaroya, H. and Wei, T. (1999), "Dynamics of transversely vibrating beams using four engineering theories", *J. Sound Vibr.*, **225**(5), 936-988.

Hanson, D, Waters, T.P., Thompson, D.J., Randall, R.B. and Ford, R.A.J. (2007), "The role of anti-resonance frequencies from operational modal analysis in finite element model updating", *Mech. Syst. Sign. Pr.*, **21**(1), 74-97.

Heyliger, P.R. and Reddy, J.N. (1988), "A higher order beam finite element for bending and vibration problems", *J. Sound Vibr.*, **126**(2), 309-326.

Holmes, M. (1961), "Steel Frames with brick work and concrete infilling", *Proceedings of the Institution of the Civil Engineers*, **19**(4), 473-478.

Holmes, M. (1963), "Combined loading on infilled frames", *Proceeding of the Institution of Civil Engineers*, **25**(1), 31-38.

Howson, W.P. and Watson, A. (2017), "Exact eigensolution of a class of multi-level elastically connected members", *Eng. Struct.*, **143**, 375-383.

Jones, K. and Turcotte, J. (2002), "Finite element model updating using antiresonant frequencies", *J. Sound Vibr.*, **252**(4), 717-727.

Klouche, F., Darcherif, L., Sekkal, M., Tounsi, A. and Mahmoud, S.R. (2017), "An original single variable shear deformation theory for buckling analysis of thick isotropic plates", *Struct. Eng. Mech.*, **63**(4), 439-446.

Labib, A., Kennedy, D. and Featherstone, C. (2014), "Free vibration analysis of beams and frames with multiple cracks for damage detection", *J. Sound Vibr.*, **333**(20), 4991-5003.

Levinson, M. (1981), "A new rectangular beam theory", *J. Sound Vibr.*, **74**(1), 81-87.

Li, H., Yin, X. and Wu, W. (2016), "Dynamic stiffness formulation for in-plane and bending vibrations of plates with two opposite edges simply supported", *J. Vibr. Contr.*, **24**(9), 1652-1669.

Lien, N. and Yao, G.C. (2000), "Identification of anti-resonance frequency in buildings based on vibration measurements", *Proceedings of the 12th World Conference on Earthquake Engineering*, Auckland.

Mainstone, R.J. (1974), *Supplementary Note on the Stiffness and Strenght of Infilled Frames*, Building Research Establishment, London, U.K.

Mei, C. (2012), "Free vibration analysis of classical single-storey multi-bay planar frames", *J. Vibr. Contr.*, **19**(13), 2022-2035.

Mei, C. (2018), "Analysis of in- and out-of plane vibrations in a rectangular frame based on two- and three dimensional

structural models", *J. Sound Vibr*., 1-28.
Mei, C. and Sha, H. (2015), "Analytical and experimental study of vibrations in simple spatial structures", *J. Vibr. Contr*., **22**(17), 3711-3735.
Miao, Y., Shi, Y., Luo, H. and Gao, R. (2018), "Closed-form solution considering the tangential effect under harmonic line load for an infinite Euler-Bernoulli beam on elastic foundation", *Appl. Math. Model*., **54**, 21-33.
Náprstek, J. and Fischer, C. (2017), "Investigation of bar system modal characteristics using dynamic stiffness matrix polynomial approximations", *Comput. Struct*., **180**, 3-12.
Ozturkoglu, O., Ucar, T. and Yesilce, Y. (2017), "Effect of masonary infill walls with openings on nonlinear response of reinforced concrete frames", *Earthq. Struct*., **12**(3), 333-347.
Paz, M. and Leigh, W. (2004), *Structural Dynamics-Theory and Computation*, Kluwer Academic Publishers, U.S.A.
Polyakov, S.V. (1950*), Investigation of the Strength and of the Deformational Characteristics of Masonry Filler Walls and facing on Framed Structures*, Construction Industry Instıtute 3.
Rao, S.S. (1995), *Mechanical Vibrations*, Addison-Wesley Publishing Company, U.S.A.
Reddy, J.N. (1984), "A simple higher-order theory for laminated composite plates", *J. Appl. Mech*., **51**(4), 745-752.
Rubio, L., Fernández-Sáez, J. and Morassi, A. (2015), "Identification of two cracks in a rod by minimal resonant and antiresonant frequency data", *Mech. Syst. Sign. Pr*., **60**, 1-13.
Salama, M.I. (2015), "Estimation of period of vibration for concrete moment-resisting frame buildings", *Hous. Build. Nat. Res. Center*, **11**(1), 16-21.
Shimpi, R.P, Patel, H.G. and Arya, H. (2007), "New first order shear deformation plate theories", *J. Appl. Mech*., **74**(3), 523-533.
Shimpi, R.P, Shetty, R.A. and Guha, A. (2017), "A simple single variable shear deformation theory for a rectangular beam", *J. Mech. Eng. Sci*., **231**(24), 4576-4591.
Shimpi, R.P. (2002), "Refined plate theory and its variants", *AIAA J*., **40**(1), 137-146.
Su, H. and Banerjee, J.R. (2015), "Development of dynamic stiffness method for free vibration of functionally graded Timoshenko beams", *Comput. Struct*., **147**, 107-116.
Tamboli, H.R. and Karadi, U.N. (2012), "Seismic analysis of RC frame structure with and without masonary infill walls", *Ind. J. Nat. Sci*., **3**(14), 1137-1194.
Tan, G., Wang, W., Cheng, Y., Wei, H., Wei, Z. and Li, H. (2018), "Dynamic response of a nonuniform Timoshenko beam with elastic supports, subjected to a moving spring-mass system", *Int. J. Struct. Stab. Dyn*., **18**(5), 1850066-1-1852266-23.
Thambiratnam, D. (2009), "Modelling and analysis of infilled frame structures under seismic loads", *Open Constr. Build. Technol. J*., **3**, 119-126.
Thinh, T.I. and Nguyen, M.C. (2016), "Dynamic stiffness matrix of continuous element for vibration of thick cross-ply laminated composite cylindrical shells", *Compos. Struct*., **98**, 93-102.
Tounsi, D., Casimir, J.B., Abid, S., Tawfiq, I. and Haddar, M. (2014), "Dynamic stiffness formulation and response analysis of stiffened shells", *Comput. Struct*., **132**, 75-83.
Zhang, C., Jin, G., Ye, T. and Zhang, Y. (2018), "Harmonic response analysis of coupled plate structures using the dynamic stiffness method", *Thin Wall Struct*., **127**, 402-415.

CC